

Comprehensive Study of the Thermochemistry of First-Row Transition Metal Compounds by Spin Component Scaled MP2 and MP3 Methods

Isabella Hyla-Kryspin and Stefan Grimme*

Organisch-Chemisches Institut der Universität Münster,
Corrensstrasse 40, D-48149 Münster, Germany

Received July 1, 2004

The enthalpies of (i) the dissociation reactions of the carbonyl ligand in $\text{Cr}(\text{CO})_n$ [$n = 6$ (**1a**), 5 (**1b**), 4 (**1c**)], $\text{Fe}(\text{CO})_5$ (**2a**), and $\text{Ni}(\text{CO})_n$ [$n = 4$ (**3a**), 3 (**3b**), 2 (**3c**)], (ii) the dissociation reactions of the heteroligand L in $\text{Cr}(\text{CO})_5\text{L}$ [L = CS (**4a**), Xe (**4b**), H_2 (**4c**), C_2H_4 (**4d**), C_2F_4 (**4e**)], $\text{Cr}(\text{CO})_3\text{L}$ [L = C_6H_6 (**5a**), C_6Me_6 (**5b**)], and $\text{Fe}(\text{CO})_4\text{L}$ [L = H_2 (**6a**), C_2H_4 (**6b**)], (iii) the deprotonation reactions of $\text{Cr}(\text{CO})_3\text{C}_6\text{H}_6$ (**5a**) and $\text{Fe}(\text{CO})_3\text{C}_4\text{H}_6$ (**8**), (iv) the protonation reaction of ferrocene (**10**), and (v) the hydrogenation reactions of $\text{Mn}_2(\text{CO})_{10}$ (**13**) and $\text{Co}_2(\text{CO})_8$ (**15**) were calculated at the DFT/BP86, MP2, MP3, SCS-MP2, and SCS-MP3 levels and compared with the corresponding experimental data. The set of systems studied covers different types of chemical bonding and a broad range of reaction enthalpies (from a few kcal/mol to a few hundred kcal/mol), and it is thus proposed as a general benchmark for quantum chemical methods. It is shown that the erratic behavior of the low-order MP approaches can be corrected by the newly developed spin component scaled perturbation theory (SCS-MP2, SCS-MP3). Both methods are based on a partitioning of the total correlation energy into contributions from antiparallel- ($\alpha\beta$) and parallel-spin ($\alpha\alpha$, $\beta\beta$) pairs of electrons, followed by a unique scaling procedure of the two correlation energy terms. The calculated thermochemical data at the SCS-MP2 and SCS-MP3 levels are significantly improved as compared to those from their standard counterparts. For the dissociation processes of **1–6** the mean absolute errors are 21.0 kcal/mol (MP2), 22.3 kcal/mol (MP3), 11.6 kcal/mol (SCS-MP2), 4.1 kcal/mol (SCS-MP3), and 3.4 kcal/mol (DFT/BP86). It is shown that contrary to standard MP3, the new SCS-MP3 method is able to predict the reaction energetics for wide variety of TM compounds with an accuracy comparable to that from DFT. The SCS-MP3 enthalpy of the hydrogenation reaction of **13** (5.8 kcal/mol) agrees better with the experiment (8.7 ± 0.3 kcal/mol) than the BP86 value (1.7 kcal/mol). The SCS-MP3 proton affinity of metal-protonated ferrocene **11** (214.8 kcal/mol) and of the agostic form **12** (203.9 kcal/mol) compare well with the experimental values (206–213 kcal/mol) and contrary to MP2 do not exclude the dynamic behavior of protonated ferrocene. It is suggested that for complex chemical systems including transition metals simultaneous application of DFT and SCS-MP3 methods may be helpful to increase the reliability of the predictions.

Introduction

The accurate calculation of the strength of chemical bonds as well as of the energetics of chemical reactions requires an accurate calculation of the electron correlation (EC) energy. In the frames of ab initio electronic structure theory there are different methods available to account for EC effects. In general, they are based on or derived from variational configuration interaction (CI), coupled-cluster (CC), and perturbation theory approaches.¹ Although a computational chemist has today a wide range of pure ab initio techniques at his or her disposal, it is still important to determine the range of systems to which these methods can be applied with the desired target accuracy.

For larger “real-life” systems that cannot be treated anymore by very accurate methods (e.g., full CI or CCSDT) a comparison of the calculated data from the chosen theoretical approach with the corresponding experimental ones is necessary to estimate the computational errors. Despite the enormous progress in quantum chemistry, it has also been recognized that in order to achieve higher accuracy an introduction of a few empirical parameters to the parameter-free ab initio methods is useful. In this spirit, approaches that use a few well-defined parameters, such as the G2-family of theories² or the hybrid density functional theory (DFT) procedures,³ were developed and belong today to the most widely used methods. In the SAC (scaling-all-correlation)⁴ or the PCI-80⁵ treatments, higher accuracy

* To whom correspondence should be addressed. E-mail: grimmes@uni-muenster.de. Tel: +49 (0)2518336512. Fax: +49 (0)2518336515.

(1) Helgaker, T.; Jørgensen, P.; Olsen, J. *Molecular Electronic Structure Theory*; Wiley: New York, 2000.

(2) (a) Curtiss, L. A.; Raghavachari, K.; Trucks, G. W.; Pople, J. A. *J. Chem. Phys.* **1991**, *94*, 7221. (b) Curtiss, L. A.; Raghavachari, K.; Pople, J. A. *J. Chem. Phys.* **1993**, *98*, 1293.

(3) Becke, A. D. *J. Chem. Phys.* **1992**, *96*, 2155.

was achieved by scaling the total correlation energy obtained from a particular wave function method by a factor that was always greater than unity. This type of scaling mainly accounts for one-particle basis set deficiencies and does not distinguish individual components of the underlying wave function.

Prior to the advent of DFT methods,^{3,6} second-order Møller–Plesset perturbation theory (MP2)⁷ was the simplest and cheapest way to incorporate EC effects in an ab initio electronic structure calculation. In recent publications we showed that a simple (cost-free) modification of the second- and third-order Møller–Plesset perturbation theories (MP2, MP3) leads to dramatic improvements of the accuracy especially for problematic systems.⁸ The new approaches termed SCS-MP2 and SCS-MP3, where SCS means spin component scaled (see below), were initially tested on a benchmark set of isogyric reactions, atomization energies, stretched geometries, difficult main group systems, and a few transition metal (TM) compounds, which are normally outside the usual applicability of low-order MP n theory.^{8a,b} The SCS-MP3 model yields results of almost QCISD(T) accuracy, which indicates that this approach accounts for higher order (mainly triples) correlation effects.⁸ From the computational point of view there are today few arguments against using low-order MP n methods even for large molecular systems. Like DFT or CC approaches they are based on a single reference (Hartree–Fock) state, and this type of wave function is well-defined and sufficient enough for many important chemical systems such as those considered here. Furthermore, MP2 and even MP3 are much faster than methods that require iterations (e.g., CISD, QCISD, CCSD) and can therefore be used with large one-particle basis sets. With efficient implementation as, for example, in the AO basis using localized orbitals,⁹ or with the resolution-of-the-identity (RI) approximation¹⁰ that is used in this work, MP3 (MP2) calculations are routinely feasible for systems with 500–1000 (2000–3000) basis functions.

It is well known that in the case of TM compounds and especially for the first-row metals, the determination of accurate bond strengths and reaction energies is a quite difficult task for both experimental and theoretical methods.^{5,11,12} Nowadays, computational TM chemistry¹³ is dominated by DFT, which provides good

results not only for geometries and vibrational frequencies but also for the energetics. Up to now, alternative ab initio methods are either too costly for large molecules [e.g., CCSD(T)] or not accurate enough. We think, however, that the study of complex chemical systems in general requires the simultaneous application of different methods in order to increase the reliability of the predictions, and thus alternatives to DFT are certainly needed.

From the applications of MP n theories to TM chemistry it is known that despite some success in determining geometries and vibrational frequencies,¹⁴ the TM–L bond energies calculated by MP2 are always too high^{13b} and the corresponding MP3 and MP4 values are often strongly oscillating.^{15a} Not much is known about the reasons for the problems of the MP n series especially for closed-shell systems with metals in low formal oxidation states. It is clear, however, that multireference (near-degeneracy) effects that are often responsible for problems with perturbation theory play only a minor role for the systems considered here.^{15b} In this paper we will show that much of the erratic behavior of the MP n methods for TM compounds can be corrected by the simple SCS ansatz and that very reliable predictions can be obtained that concur with DFT results. For that purpose we developed a thermochemical “benchmark” set of TM systems and reactions for which experimental data are reasonably well known. For a limited number of TM systems, the improved performance of the new SCS-MP2 and SCS-MP3 methods compared to MP2 and MP3 has been noted before^{8a,b} although a more detailed study on “realistic” examples is definitely warranted. Thus, in the present study we investigate (i) the dissociation energies of the carbonyl ligand in Cr(CO) $_n$ [$n = 6$ (**1a**), 5 (**1b**), 4 (**1c**)], Fe(CO) $_5$ (**2a**), and Ni(CO) $_n$ [$n = 4$ (**3a**), 3 (**3b**), 2 (**3c**)], (ii) the dissociation energies of the heteroligand L in Cr(CO) $_5$ L [L = CS (**4a**), Xe (**4b**), H $_2$ (**4c**), C $_2$ H $_4$ (**4d**), C $_2$ F $_4$ (**4e**)], Cr(CO) $_3$ L [L = C $_6$ H $_6$ (**5a**), C $_6$ Me $_6$ (**5b**)], and Fe(CO) $_4$ L [L = H $_2$ (**6a**), C $_2$ H $_4$ (**6b**)], (iii) the deprotonation reaction of Cr(CO) $_3$ C $_6$ H $_6$ (**5a**) and Fe(CO) $_3$ C $_4$ H $_6$ (**8**), (iv) the proton affinity of ferrocene (**10**), and (v) the hydrogenation reaction of Mn $_2$ (CO) $_{10}$ (**13**) and Co $_2$ (CO) $_8$ (**15**). This choice not only covers a broad range of reaction energies, i.e., from a few kcal/mol to a few hundred kcal/mol, but also takes into account different types of chemical bonding. A standard DFT method is also applied in order to put the results of the SCS-MP n methods in a more solid perspective. In some cases where the errors of the reference experimental data are large, comparison with the DFT data will also help to assess the quality of the results.

Computational Details

The geometry optimizations of the complexes, metal-containing fragments, and ligands were carried out at the DFT/

(4) Gordon, M. S.; Truhlar, D. G. *J. Am. Chem. Soc.* **1986**, *108*, 5412.

(5) (a) Siegbahn, P. E. M.; Blomberg, M. R. A.; Svensson, M. *Chem. Phys. Lett.* **1994**, *223*, 35. (b) Siegbahn, P. E. M.; Svensson, M.; Boussard, P. J. E. *J. Chem. Phys.* **1995**, *102*, 5377. (c) Blomberg, M. R. A.; Siegbahn, P. E. M.; Svensson, M. *J. Chem. Phys.* **1996**, *104*, 9546.

(6) Parr, R. G.; Yang, W. *Density-Functional Theory of Atoms and Molecules*; Oxford University Press: Oxford, 1989.

(7) (a) Møller, C.; Plesset, M. S. *Phys. Rev.* **1934**, *46*, 618. (b) Cremer, D. In *Encyclopedia of Computational Chemistry*; Schleyer, P. v. R., Ed.; Wiley: New York, 1998; p 1706. (c) Bartlett, R. J. *J. Chem. Phys.* **1975**, *62*, 3258. (d) Pople, J. A.; Binkley, J. S.; Seeger, R. *Int. J. Quantum Chem. Symp.* **1976**, *10*, 1.

(8) (a) Grimme, S. *J. Chem. Phys.* **2003**, *118*, 9095. (b) Grimme, S. *J. Comput. Chem.* **2003**, *24*, 1529. (c) Piacenza, M.; Grimme, S. *J. Comput. Chem.* **2004**, *25*, 83. (d) Grimme, S.; Gerenkamp, M. *Chem. Phys. Lett.* **2004**, *392*, 229.

(9) Schütz, M.; Lindh, R.; Werner, H.-J. *J. Mol. Phys.* **1999**, *96*, 719.

(10) (a) Vahtras, O.; Almlöf, J.; Feyereisen, M. W. *Chem. Phys. Lett.* **1993**, *213*, 514. (b) Weigend, F.; Häser, M. *Theor. Chem. Acc.* **1997**, *97*, 331.

(11) (a) Martinho-Simões, J. A.; Beauchamp, J. L. *Chem. Rev.* **1990**, *90*, 629. (b) Nolan, P. In *Encyclopedia of Inorganic Chemistry*; King, R. B., Ed.; Wiley: New York, 1994; Vol. 1.

(12) (a) Veillard, A. *Chem. Rev.* **1991**, *91*, 743. (b) Davidson, E. R. In *The Challenge of d and f Electrons—Theory and Computation*; Salahub, D. R., Zerner, M. C., Eds.; ACS Symposium Series 394; American Chemical Society, Washington, DC, 1989; pp 153–164.

(13) (a) Ziegler, T. *Chem. Rev.* **1991**, *91*, 651. (b) Frenking, G. Wagoner, T. In *Encyclopedia of Computational Chemistry*; Schleyer, P. v. R., Ed.; Wiley: New York, 1998; pp 3073–3084.

(14) (a) Jonas, V.; Thiel, W. *J. Chem. Phys.* **1995**, *102*, 8474. (b) Jonas, V.; Thiel, W. *J. Chem. Phys.* **1996**, *105*, 3636.

(15) (a) Hyla-Kryspin, I.; Koch, J.; Gleiter, R.; Klettke, T.; Walther, D. *Organometallics*, **1998**, *17*, 4724. (b) Most of the systems studied are colorless and thus have no low-lying excited states. The HOMO–LUMO gaps are typically large, i.e., >7–8 eV at the HF level of theory.

BP86 level¹⁶ by using the RI approximation¹⁷ for the Coulomb operator. In all DFT and HF calculations the TURBOMOLE suite of programs^{18,19} was used. With the exception of Xe all atoms were described with all-electron valence triple- ξ Gaussian basis sets augmented with polarization functions: (17s11p6d1f)/(6s4p3d1f) for TM, (11s6p2d)/(5s3p2d) for C, O, F, (14s9p2d)/(5s5p2d) for S, and (6s2p)/(3s2p) for H. In the case of the Xe atom 46 core electrons were approximated by pseudopotentials²⁰ and the valence electrons were described by a (6s6p2d1f)/(4s4p2d1f) basis. Single-point MP2 and MP3 calculations were performed with the same basis sets on the RIDFT/BP86 optimized structures by using the RICC program developed in our laboratory.²¹ This code uses the RI approximation, and it is integral-direct and specially designed to run in parallel on mass-market PCs or PC clusters. All mentioned basis sets together with the auxiliary basis sets for the RI approximation (jbasen for DFT/BP86 and cbasen for MP2 and MP3) were taken from the TURBOMOLE basis set library.²² Note that the AO basis sets used here (especially for the larger systems) are of significantly higher quality than those used in most previous computational studies on TM compounds. The basis set convergence of the calculated reaction energies has been tested for the representative systems **1c**, **3a**, **6a**, and **6b** by employing even larger polarized quadruple- ξ basis sets for the ligands {C, O: (15s8p3d2f1g)/[7s4p3d2f1g]; H: (7s3p2d1f)/[4s3p2d1f]} and an additional f-function for the metal ($\alpha_{\text{p}} = 0.5\alpha_{\text{d}}$). The results obtained differ by less than 0.5 kcal/mol (DFT) and 0.1–3.4 kcal/mol (SCS-MP n), respectively, from the data obtained with our standard basis, indicating sufficient convergence and the reliability of our conclusions (for details see the Discussion section). According to prior experience, the errors due to the RI approximation are less than 0.01% and 0.02 kcal/mol for the absolute correlation energies and relative energies, respectively. In the MP2 and MP3 correlation treatments only valence electrons (3s3p shells are included for TM) were considered, and thus core–core and core–valence correlation effects are completely neglected. These contributions are known to reach up to 0.5 kcal/mol for simple reactions involving molecules composed of first-row elements.²³ For the systems studied here, the errors due to this frozen-core approximation may reach 1–2 kcal/mol. However, taking into account that the experimental uncertainties concerning the thermochemistry of TM compounds are usually about 2–5 kcal/mol and reaching sometimes 15 kcal/mol,²⁴ the errors introduced by RI and frozen core approximations may be regarded as negligible.

The SCS-MP2 and SCS-MP3 models are based on a partitioning of the correlation energy, $E_{\text{c}} = E_{\text{exact}} - E_{\text{HF}}$, into contributions from antiparallel- ($\alpha\beta$) and parallel-spin ($\alpha\alpha, \beta\beta$) pairs of electrons, i.e., $E_{\text{c}} = E_{\text{T}} + E_{\text{S}}$.^{8a,b} We observed that if

(16) (a) Becke, A. D. *Phys. Rev. A* **1988**, *38*, 3098. (b) Perdew, J. P. *Phys. Rev. B* **1986**, *33*, 8822.

(17) (a) Eichkorn, K.; Treutler, O.; Öhm, H.; Häser, M.; Ahlrichs, R. *Chem. Phys. Lett.* **1995**, *242*, 652. (b) Treutler, O.; Ahlrichs, R. *J. Chem. Phys.* **1995**, *102*, 346.

(18) Ahlrichs, R.; Bär, M.; Baron, H.-P.; Bauernschmitt, R.; Böcker, S.; Ehrig, M.; Eichkorn, K.; Elliot, S.; Furche, F.; Haase, F.; Häser, M.; Horn, H.; Huber, C.; Huniar, U.; Kattannek, M.; Kölmel, C.; Kollwitz, M.; May, K.; Ochsenfeld, C.; Öhm, H.; Schäfer, A.; Schneider, U.; Treutler, O.; von Arnim, M.; Weigend, F.; Weis, P.; Weiss, H. *TURBOMOLE*, Ver. 5.6; Universität Karlsruhe, 2003.

(19) von Arnim, M.; Ahlrichs, R. *J. Comput. Chem.* **1998**, *19*, 1746.

(20) Nicklass, A.; Dolg, M.; Stoll, H.; Preuss, H. *J. Chem. Phys.* **1995**, *102*, 8942.

(21) Grimme, S.; Izgorodina, E. *RICC: A coupled-cluster program using the RI approximation*; University of Münster, 2002.

(22) The basis sets are available from the TURBOMOLE homepage <http://www.turbomole.com> via FTP Server Button in the subdirectories basen, jbasen (auxiliary basis set for RIDFT calculations) and cbasen (auxiliary basis sets for RIMP n calculations).

(23) Bak, K. L.; Jørgensen, P.; Olsen, J.; Helgaker, T.; Klopper, W. *J. Chem. Phys.* **2000**, *112*, 9229.

(24) NIST Standard Reference Database. See <http://webbook.nist.gov/chemistry/>.

the pair energies are estimated by MP2, the E_{T} contribution which partially accounts for long-range (static) correlation effects is overestimated, while the E_{S} part is underestimated. In ref 8a we introduced a scaling scheme according to eq 1:

$$E_{\text{c}} \approx E_{\text{c}}^{\text{SCS-MP2}} = p_{\text{S}}E_{\text{S}}^{(2)} + p_{\text{T}}E_{\text{T}}^{(2)} \quad (1)$$

where p_{S} and p_{T} are system-independent scaling parameters ($p_{\text{S}} = 6/5$, $p_{\text{T}} = 1/3$). Since the SCS-MP2 energy already contains some of the higher order effects, the usual MP n corrections ($n > 2$) must be damped. In ref 8b we proposed to use

$$E_{\text{c}}^{\text{SCS-MP3}} = E_{\text{c}}^{\text{SCS-MP2}} + p_3E^{(3)} \quad (2)$$

as an estimate for the correlation energy, where p_3 is an additional scaling parameter and $E^{(3)}$ is the usual third-order correction evaluated with the (unscaled) first-order amplitudes. For explicit formulas of the $E^{(3)}$ and $E^{(2)}$ corrections, see, for example, refs 8a,b and 25. The parameter p_3 was determined empirically on a large and diverse benchmark set of molecules ($p_3 = 1/4$).^{8b} Note, that the SCS energies can be obtained from any standard quantum chemical program package (e.g., GAUSSIAN) that can do MP2/MP3 calculations simply by applying the necessary scaling to the corresponding correlation energy contributions.

Reaction enthalpies, $\Delta H_{\text{R}}(\text{calc})$, were calculated with the differences between the total electronic energies (E_{elec}), zero-point-vibrational-energy (ZPVE), and thermal energies (E_{th}) of the products and reactants and corrected for the volume work [$\Delta(PV)$] term (eq 3).²⁶

$$\Delta H_{\text{R}}(\text{calc}) = \Delta E_{\text{elec}} + \Delta \text{ZPVE} + \Delta E_{\text{th}} + \Delta(PV) \quad (3)$$

Zero-point energies were obtained from harmonic vibrational frequencies (unscaled) obtained at the DFT/BP86 level by using the SNF program.²⁷ The thermal energy contributions (ΔE_{th}) correspond to the sum of the changes in translational, rotational, and vibrational energies when going from 0 to 298.15 K. For the volume work term we assume ideal gas behavior, and thus it is equal to ΔnRT .²⁶ Experimental reaction enthalpies $\Delta H_{\text{R}}(\text{exp})$ were either taken directly from the available experimental data or calculated from standard enthalpies of formation ($\Delta H_{\text{f}}^{\circ}$) of the involved species.²⁴

Results and Discussion

A. Enthalpies of the Dissociation Reactions of the Carbonyl Ligand in Homoleptic Metal Carbonyls of Cr(1), Fe(2), and Ni(3). Due to their importance in industry for homogeneous and heterogeneous catalysis as well as for synthesis in academic research (see, for example, refs 28a–d and references therein), TM carbonyls belong to the most studied compounds. For theoretical TM chemistry they constitute a small but widely used “benchmark set” for an evaluation of the accuracy and/or calibration of newly developed or improved methods. The molecular structures, bonding

(25) Krishnan, R.; Pople, J. A. *Int. J. Quantum Chem.* **1978**, *14*, 91.

(26) (a) Del Bene, J. E. In *Molecular Structure and Energetics: Bonding Models*; Liebmann, J. F., Greenberg, A., Eds.; VCH: Deerfield Beach, FL, 1986; Vol. 1, pp 319–349. (b) Pitzer, K. S. *Quantum Chemistry*; Prentice-Hall: Englewood Cliffs, NJ, 1961.

(27) Kind, C.; Reiher, M.; Neugebauer, J.; Hess, B. A. *SNF (Vers.2.2.1)*, A program for numerical frequency analyses; University of Erlangen, 2002.

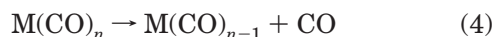
(28) (a) W. Parshall, G. W. *J. Mol. Catal.* **1978**, *3*, 243. (b) Masters, C. *Homogeneous Transition-Metal Catalysis—A Gentle Art*; Chapman and Hall: London, 1981. (c) Guzzi, L. *Studies in Surface Science and Catalysis*, Vol. 64: *New Trends of CO Activation*; Elsevier: Amsterdam, 1991. (d) Elschenbroich, Ch.; Salzer, A. *Organometallics A Concise Introduction*, 2nd ed.; VCH: Weinheim, Germany, 1992.

Table 1. Theoretically Predicted and Experimentally Observed Enthalpies of the Dissociation Reactions of the Carbonyl Ligands in Homoleptic Metal Carbonyls of Chromium, Iron, and Nickel^a

dissociation process	$\Delta H_R(\text{calc})$ [kcal/mol]					$\Delta H_R(\text{exp})$ [kcal/mol]	ref
	BP86	MP2	MP3	SCS-MP2	SCS-MP3		
1a: Cr(CO) ₆ → CrCO ₅ + CO	40.4 (+3.3)	58.6 (+21.5)	17.4 (−19.7)	49.1 (+12.0)	38.8 (+1.7)	<i>37.1 ± 5.0; 36.8 ± 3.1;</i> 37.7	30
1b: Cr(CO) ₅ → Cr(CO) ₄ + CO	39.3 (+6.3)	45.5 (+12.5)	24.4 (−8.6)	38.7 (+5.7)	33.4 (+0.4)	<i>33.0; 40.0 ± 15.0;</i> 25.1 ± 5.0	30a, 31
1c: Cr(CO) ₄ → Cr(CO) ₃ + CO	40.1 (+1.1)	49.9 (+10.9)	21.8 (−17.2)	42.8 (+3.8)	35.9 (−3.1)	<i>39.0; 20.1 ± 15.0</i>	30
2a: Fe(CO) ₅ → Fe(CO) ₄ + CO	44.2 (+2.6)	69.2 (+27.6)	9.3 (−32.3)	52.9 (+11.3)	39.9 (−1.7)	<i>41.6 ± 3.1; 55.5 ± 11.5</i>	30b,32
3a: Ni(CO) ₄ → Ni(CO) ₃ + CO	27.2 (+2.3)	53.2 (+28.3)	−41.7 (−66.6)	41.3 (+16.4)	17.5 (−7.4)	<i>24.9 ± 1.9</i>	33
3b: Ni(CO) ₃ → Ni(CO) ₂ + CO	37.1 (+8.8)	53.6 (+25.3)	0.5 (−27.8)	45.6 (+17.3)	32.3 (+4.0)	<i>28.3 ± 2.3; 13.2 ± 10.0</i>	33, 34
3c: Ni(CO) ₂ → Ni(CO) + CO	54.4 (+7.3)	55.9 (+8.8)	10.4 (−36.7)	48.2 (+1.1)	39.1 (−8.0)	<i>47.1 ± 5.7; 54.5 ± 15.1</i>	33, 34
MAE ^b	4.5	19.3	29.8	9.6	3.7		

^a Computational errors with respect to the most reliable experimental data (printed in italics) are given in parentheses. ^b Mean absolute error.

energies, and spectroscopic properties of **1–3** have been investigated with almost all known methods and discussed in several independent studies.^{5c,14,15,29} In Table 1 we present the SCS-MP2 and SCS-MP3 dissociation enthalpies for the process



[M = Cr: $n = 6$ (**1a**), 5 (**1b**), 4 (**1c**); M = Fe: $n = 5$ (**2a**); M = Ni: $n = 4$ (**3a**), 3 (**3b**), 2 (**3c**)] in comparison with DFT/BP86, MP2, MP3, and experimental results.^{30–34}

In all our calculations we have assumed a spin-allowed dissociation process; that is, only singlet states of the involved species are considered. This is true for CO dissociation from **1a–1c** and **3a–3c**, but in the case of **2a** the resulting Fe(CO)₄ fragment is known experimentally to have a triplet ground state.³⁵ The calculated singlet–triplet energy splitting of Fe(CO)₄ varies from a few kcal/mol^{29e,k} to some dozen kcal/mol,^{29j,36} depend-

ing on the method used for calculation (the experimental value is not known). It should be noticed, however, that according to the discussion concerning the experimentally measured first CO dissociation enthalpy of **2a**, the determined value of 41.6 ± 3.1 kcal/mol corresponds to a spin-allowed process.^{30b}

From the previous studies on **1a–3a** it is known that the BP86 functional provides rather accurate results for both the dissociation energies and the molecular structures.^{14a,29e,f,k} This is the main reason to employ the BP86 method for geometry optimization in the present work. The optimized M–C and C–O bond distances of **1–3** are compared with the available experimental data in Table 2.

As can be seen from Table 2, the BP86 optimized structures are in very good agreement with those from experiment³⁷ and previous calculations.^{14a,29e,f,k} The dissociation enthalpies of the carbonyl ligand are in general slightly overestimated by BP86,^{29e,f,k} which is also confirmed by our studies (Table 1). Other functionals (e.g., B88-VWN, B88-LYP, or B3LYP) underestimate the M–CO bond strengths.^{15,29d,j,k,q} For the seven CO dissociation processes, the largest deviation of BP86 from experiment is +8.8 kcal/mol [for CO dissociation from Ni(CO)₃] and the mean absolute error (MAE) amounts to 4.5 kcal/mol (Table 1). As expected, the MP2 and MP3 dissociation enthalpies clearly show the inability of both methods to properly describe the M–CO bond strengths. With respect to the experimental data all MP2 values are too large, while MP3 underestimates the energies and shows a behavior similar to that of HF, indicating an oscillatorial behavior of the MP series.^{29b} The data in Table 1 clearly demonstrate that both SCS-MP2 and SCS-MP3 significantly improve upon their standard counterparts. The largest deviations at the MP2 and MP3 levels occur for Ni(CO)₄ and amount to +28.3 kcal/mol (MP2) and −66.6 kcal/mol (MP3), and by the SCS approach these values diminish to +16.4 and −7.4 kcal/mol, respectively. It is seen that SCS-MP3 is superior over SCS-MP2, which is exactly opposite of MP3 and MP2. Upon going from MP2 to MP3, the MAE increases from 19.3 kcal/mol to 29.8 kcal/mol, while for the SCS-MP2/SCS-MP3 pair the MAE decreases from 9.6 kcal/mol to 3.4 kcal/mol. Thus for this set of reactions

(29) (a) Barnes, L. A.; Liu, B.; Lindh, R. *J. Chem. Phys.* **1993**, *98*, 3978. (b) Ehlers, A. W.; Frenking, G. *J. Am. Chem. Soc.* **1994**, *116*, 1514. (c) Persson, B. J.; Roos, B. O.; Pierloot, K. *J. Chem. Phys.* **1994**, *101*, 6810. (d) Delley, B.; Wrinn, M.; Lüthi, H. P. *J. Chem. Phys.* **1994**, *100*, 5785. (e) Li, J.; Schreckenbach, G.; Ziegler, T. *J. Am. Chem. Soc.* **1995**, *117*, 486. (f) van Wüllen, C. *J. Chem. Phys.* **1996**, *105*, 5485. (g) Demuyneck, J.; Strich, A.; Veillard, A. *Nouv. J. Chim.* **1977**, *1*, 217. (h) Lüthi, H. P.; Siegbahn, P. E. M.; Almlöf, J. A. *J. Phys. Chem.* **1985**, *89*, 2156. (i) Ehlers, A. W.; Frenking, G. *Organometallics* **1995**, *14*, 423. (j) Barnes, L. A.; Rosi, M.; Bauschlicher, C. W., Jr. *J. Chem. Phys.* **1991**, *94*, 2031. (k) González-Blanco, O.; Branchadell, C. *J. Chem. Phys.* **1999**, *110*, 778. (l) Wang, W.; Weitz, E. *J. Phys. Chem. A* **1997**, *101*, 2358. (m) Rohlfing, C. M.; Hay, P. J. *J. Chem. Phys.* **1985**, *82*, 270. (n) Blomberg, M. R. A.; Siegbahn, P. E. M.; Lee, T. J.; Rendell, A. P.; Rice, J. E. *J. Chem. Phys.* **1991**, *95*, 5898. (o) Blomberg, M. R. A.; Brandemark, U. B.; Siegbahn, P. E. M.; Wennerberg, J.; Bauschlicher, C. W., Jr. *J. Am. Chem. Soc.* **1988**, *110*, 6650. (p) Bauschlicher, C. W., Jr.; Langhoff, S. R. *Chem. Phys.* **1989**, *129*, 431. (q) Chen, Y.; Hartmann, M.; Frenking, G. *Z. Anorg. Allg. Chem.* **2001**, *627*, 985. (r) Liang, B.; Zhou, M.; Andrews, L. *J. Phys. Chem. A* **2000**, *104*, 3905.

(30) (a) Fletcher, R. T.; Rosenfeld, R. N. *J. Am. Chem. Soc.* **1988**, *110*, 2097. (b) Lewis, K. E.; Golden, D. M.; Smith, G. P. *J. Am. Chem. Soc.* **1984**, *106*, 3905. (c) Pajaro, G.; Calderazzo, F.; Ercoli, R. *Gazz. Chim. Ital.* **1960**, *90*, 1486.

(31) (a) Rayner, D. M.; Ishikawa, Y.; Brown, C. E.; Hackett, P. A. *J. Chem. Phys.* **1991**, *94*, 5471. (b) Venkataraman, B.; Hou, H.; Zhang, Z.; Chen, S.; Bandukwalla, G.; Vernon, M. *J. Chem. Phys.* **1990**, *92*, 5338.

(32) Engelking, P. C.; Lineberger, W. C. *J. Am. Chem. Soc.* **1979**, *101*, 5569.

(33) Stevens, A. E.; Feigerle, S. S.; Lineberger, W. C. *J. Am. Chem. Soc.* **1982**, *104*, 5026.

(34) Sunderlin, L. S.; Wang, D.; Squires, R. R. *J. Am. Chem. Soc.* **1992**, *114*, 2788.

(35) (a) Poliakoff, M.; Weitz, E. *Acc. Chem. Res.* **1987**, *20*, 408. (b) Poliakoff, M.; Turner, J. J. *J. Chem. Dalton Trans.* **1974**, 2278. (c) Barton, T. J.; Grinter, R.; Thompson, J.; Davies, B.; Poliakoff, M. *J. Chem. Soc., Chem. Commun.* **1977**, 841.

(36) Daniel, C.; Benard, M.; Dedieu, A.; Wiest, R.; Veillard, A. *J. Phys. Chem.* **1984**, *88*, 4805.

(37) (a) Jost, A.; Rees, B.; Yelon, W. B. *Acta Crystallogr. Sect. B* **1975**, *31*, 2649. (b) Rees, B.; Mitschler, A. *J. Am. Chem. Soc.* **1976**, *98*, 7918. (c) Braga, D.; Grepioni, F.; Orpen, A. G. *Organometallics* **1993**, *12*, 1481. (d) Beagley, B.; Schmidling, D. G. *J. Mol. Struct.* **1974**, *22*, 466. (e) Hedberg, L.; Ijima, T.; Hedberg, K. *J. Chem. Phys.* **1979**, *70*, 3224.

Table 2. Optimized Bond Lengths (Å) of Cr(CO)₆, Fe(CO)₅, Ni(CO)₄, and Their Most Stable Molecular Fragments in the Singlet State (available experimental data given in parentheses)

	symm.	state	$R(M-C)_{ax}$	$R(M-C)_{eq}$	$R(C-O)_{ax}$	$R(C-O)_{eq}$
Cr(CO) ₆ (1a)	O_h	$^1A_{1g}$	1.910 (1.914) ^a (1.916) ^b		1.153 (1.140) ^a (1.140) ^b	
Cr(CO) ₅ (1b)	C_{4v}	1A_1	1.858	1.929	1.147	1.141
Cr(CO) ₄ (1c)	C_{2v}	1A_1	1.903	1.815	1.158	1.165
Cr(CO) ₃ (1d)	C_{3v}	1A_1	1.797		1.171	
Fe(CO) ₅ (2a)	D_{3h}	$^1A_1'$	1.810 (1.811) ^c (1.807) ^d	1.809 (1.803) ^c (1.827) ^d	1.152 (1.117) ^c (1.152) ^d	1.555 (1.133) ^c (1.152) ^d
Fe(CO) ₄ (2b)	C_{2v}	1A_1	1.813	1.778	1.154	1.160
Ni(CO) ₄ (3a)	T_d	1A_1	1.828 (1.838) ^e (1.817) ^c		1.149 (1.141) ^e (1.127) ^c	
Ni(CO) ₃ (3b)	D_{3h}	$^1A_1'$		1.804		1.152
Ni(CO) ₂ (3c)	C_{2v}	1A_1	1.758		1.157	
NiCO (3d)	$C_{\infty v}$	$^1\Sigma_g^-$	1.656		1.169	

^a Neutron diffraction, ref 37a. ^b X-ray, ref 37b. ^c X-ray, ref 37c. ^d Gas-phase electron diffraction, ref 37d. ^e Gas-phase electron diffraction, ref 37e.

Table 3. Theoretically Predicted and Experimentally Observed Enthalpies of the Dissociation Reactions of the Heteroligands L in the Carbonyl Complexes Cr(CO)₅L [L = CS (4a**), Xe (**4b**), H₂ (**4c**), C₂H₄ (**4d**), C₂F₄ (**4e**)], Cr(CO)₃L [L = C₆H₆ (**5a**), C₆Me₆ (**5b**)], and Fe(CO)₄L [L = H₂ (**6a**), C₂H₄ (**6b**)]^a**

dissociation process	$\Delta H_R(\text{calc})$ [kcal/mol]					$\Delta H_R(\text{exp})$ [kcal/mol]	ref
	BP86	MP2	MP3	SCS-MP2	SCS-MP3		
4a: Cr(CO) ₅ CS → Cr(CO) ₅ + CS	56.6 (+0.6)	84.6 (+28.6)	20.1 (−35.9)	72.5 (+16.5)	56.3 (+0.3)	56.0 ± 4.0	38a
4b: Cr(CO) ₅ Xe → Cr(CO) ₅ + Xe	4.5 (−4.5)	14.4 (+5.4)	0.3 (−8.7)	10.9 (+1.9)	7.4 (−1.6)	9.0 ± 0.9	38b
4c: Cr(CO) ₅ H ₂ → Cr(CO) ₅ + H ₂	15.2 (+0.2)	27.1 (+12.1)	9.1 (−5.9)	21.7 (+6.7)	17.2 (+2.2)	15.0 ± 1.3	38c
4d: Cr(CO) ₅ C ₂ H ₄ → Cr(CO) ₅ + C ₂ H ₄	21.6 (−3.3)	46.1 (+21.3)	6.1 (−18.8)	35.9 (+11.1)	25.9 (+1.1)	24.6 ± 3.4; 25.1 ± 1.0	38c,d
4e: Cr(CO) ₅ C ₂ F ₄ → Cr(CO) ₅ + C ₂ F ₄	16.0 (−3.7)	28.2 (+8.5)	18.7 (−1.0)	20.8 (+1.1)	18.4 (−1.3)	19.7 ± 1.4	38c
5a: Cr(CO) ₃ C ₆ H ₆ → Cr(CO) ₃ + C ₆ H ₆	58.7 (−0.8)	107.1 (+47.5)	31.9 (−27.7)	90.3 (+30.7)	71.5 (+11.9)	59.6 ± 12.3	24
5b: Cr(CO) ₃ C ₆ Me ₆ → Cr(CO) ₃ + C ₆ Me ₆	61.8 (−7.2)	122.4 (+53.5)	34.4 (−34.6)	103.1 (+34.2)	81.1 (+12.2)	66.2 ± 13.7; 71.7 ± 14.0	24, 39
6a: Fe(CO) ₄ H ₂ → Fe(CO) ₄ + H ₂	19.6 (−1.1)	27.4 (+8.9)	17.2 (−1.3)	22.6 (+3.8)	20.1 (+1.6)	18.5 ^b	
6b: Fe(CO) ₄ C ₂ H ₄ → Fe(CO) ₄ + C ₂ H ₄	31.6 (−0.6)	23.7 (−8.5)	45.8 (+13.6)	19.7 (−12.5)	25.2 (−7.0)	23.1; 37.4; 36.0 ± 2.5	30b, 40a,b
MAE ^c	2.4 (2.0)	21.6 (13.3)	16.4 (12.2)	13.2 (7.7)	4.4 (2.2)		

^a Computational errors with respect to the experimental data (mean values for reaction of **4d**, **5b**, and **6b**) are given in parentheses. ^b CCSD(T) value from ref 29q. ^c Mean absolute error, values in parentheses refer to reactions of **4a–4e** and of **6a** and **6b**.

SCS-MP3 is even slightly better than BP86. The CO dissociation energies of **1a–3a** have been the subject of higher level theoretical studies.^{29a–c,i,q} Thus, for example, CCSD(T)/MP2 overestimates the ΔH^{298} of **1a** and **2a** by 8.2 and 4.9 kcal/mol, respectively.^{29b,i} For comparison the SCS-MP3 deviations are 1.7 kcal/mol (**1a**) and −2.1 kcal/mol (**2a**) (Table 1). Probably the most accurate study for complexes **3** was done at the CASPT2 level.^{29c} The authors found that the computed Ni–CO bond energy (D_0) of **3a** (24.7 kcal/mol)^{5c,29c} almost exactly reproduces the experimental value (24.9 kcal/mol).³³ The SCS-MP3 method underestimates this dissociation enthalpy by as much as 7.4 kcal/mol (Table 1), which can be traced back partially to a basis set effect in this case (see below). However, the calculated dissociation enthalpies for **3b** [34.7 kcal/mol (CASPT2),^{5c,29c} 32.3 kcal/mol (SCS-MP3)] and **3c** [39.1 kcal/mol (CASPT2),^{5c,29c} 39.1 kcal/mol (SCS-MP3)] are of the same accuracy with respect to the experimental values [28.3 ± 2.3 kcal/mol (**3b**), 47.1 ± 5.7 kcal/mol (**3c**)].³⁴ In summary, contrary to low-order MP n theory, SCS-MP3 is able to predict the CO dissociation enthalpies of **1–3** with an accuracy comparable to that from DFT or other high-level theoretical methods.

Before continuing, we briefly want to discuss possible basis set effects for two selected examples. The use of quadruple- ξ basis for the ligands and one additional

f-function for TM does not change the BP86 dissociation reaction enthalpy of **3a**. However, the SCS-MP3 enthalpy (20.6 kcal/mol) is corrected in the right direction; that is, the deviation from experiment diminishes from 7.4 kcal/mol (Table 1) to 4.3 kcal/mol with the larger basis set. The same is valid for **1c**, for which the SCS-MP3 dissociation reaction enthalpy (38.4 kcal/mol) differs now by only 0.6 kcal/mol from the experimental value.

B. Enthalpies of the Dissociation Reactions of the Heteroligands in Cr(CO)₅L (4**), Cr(CO)₃L (**5**), and Fe(CO)₄L (**6**).** The calculated enthalpies of the dissociation reactions of the heteroligands L (eqs 5–7) are collected in Table 3.



For the sake of clarity the molecular structures of the investigated complexes **4–6** are schematically depicted in Figure 1.

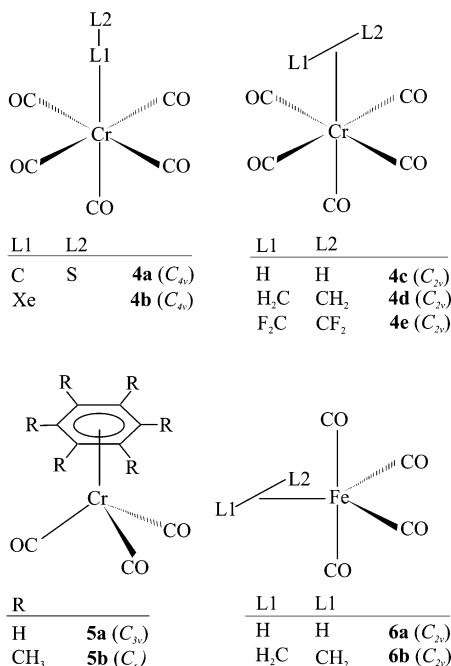
Table 4 presents selected optimized parameters of **4–6** in comparison with experimental and previous theoretical results, where available. The optimized

Table 4. Comparison of Selected Optimized Bond Distances [Å] of 4–6 with Available Theoretical and Experimental Data

	method	M–CO _{ax}	M–CO _{eq}	M–L1	L1–L2	ref
Cr(CO) ₅ CS 4a (<i>C</i> _{4v})	MP2	1.920	1.860	1.804	1.564	41a
	BP86	1.931	1.912	1.879	1.561	this work
	expt ^a			1.854	1.565	42a
Cr(CO) ₅ Xe 4b (<i>C</i> _{4v})	BP86	1.829	1.898	2.957		this work
Cr(CO) ₅ H ₂ 4c (<i>C</i> _{2v})	MP2	1.787	1.864/1.859 ^b	1.745	0.813	41a,b
	BP86	1.870	1.905/1.907 ^b	1.771	0.825	this work
Cr(CO) ₅ C ₂ H ₄ 4d (<i>C</i> _{2v})	BP86	1.867	1.906/1.902 ^b	2.333	1.384	this work
Cr(CO) ₅ C ₂ F ₄ 4e (<i>C</i> _{2v})	BP86	1.899	1.910/1.913 ^b	2.208	1.417	this work
Fe(CO) ₄ H ₂ 6a (<i>C</i> _{2v})	B3LYP	1.818	1.794	1.602	0.894	29q
	BP86	1.809	1.798	1.607	0.922	this work
	BPW91	1.782	1.791	1.525		42b
	expt ^c	1.818(1.815)	1.815(1.798)	1.576(1.590)		42b
	expt ^d	1.832	1.802	1.556		42c
Fe(CO) ₄ C ₂ H ₄ 6b (<i>C</i> _{2v})	B3LYP	1.815	1.791	2.145	1.407	29q
	BP86	1.807	1.797	2.142	1.411	this work
	BPW91	1.801	1.787	2.119	1.419	42d
	expt ^c	1.815	1.806	2.117	1.419	42d
	expt ^d	1.796	1.836	2.117	1.460	42e

	method	Cr–CO	Cr–C ₆	C ₆ –C ₆	C ₆ –C _H ₃	ref
Cr(CO) ₃ C ₆ H ₅ 5a (<i>C</i> _{3v})	BP86	1.847	2.228/2.229	1.409/1.426		this work
	expt ^e	1.876	2.180	1.406/1.422		43a
	expt ^e	1.845	2.223–2.243	1.407/1.423		43b
	expt ^f	1.845	2.220–2.243	1.495/1.423		43b
Cr(CO) ₅ C ₆ (CH ₃) ₆ 5b (<i>C</i> _s)	BP86	1.835/1.837	2.240–2.272	1.422/1.442	1.510–1.513	this work
	expt ^f	1.832/1.838	2.236–2.250	1.413/1.434	1.502–1.512	43d

^a Estimated values on the basis of experimental bond lengths of other carbonyl and thiocarbonyl complexes. ^b The first value refers to the carbonyl groups eclipsing the heteroligand. ^c Structural parameters from a least-squares fit to the rotational constants from the measured microwave spectra; values in parentheses refer to the Kraitchman analysis. ^d Gas-phase electron diffraction. ^e Neutron diffraction. ^f X-ray.

**Figure 1.** Molecular shapes of the complexes **4**, **5**, and **6**.

structures of Cr(CO)₅CS (**4a**) and Cr(CO)₅Xe (**4b**) adopt *C*_{4v} symmetry and those of Cr(CO)₅H₂ (**4c**), Cr(CO)₅C₂H₄ (**4d**), and Cr(CO)₅C₂F₄ (**4e**) as well as of Fe(CO)₄H₂ (**6a**) and Fe(CO)₄C₂H₄ (**6b**) are *C*_{2v} symmetric. In **4c**–**4e** the heteroligands have an eclipsed position with regard to cis CO groups. To our best knowledge, experimental structural data of **4a**–**4e** are not known.

There can be different conformations of the Fe(CO)₄L complexes **6**, where the heteroligand may occupy an equatorial or an axial position. In accord with the

experimental structural data^{42b–e} our calculations were carried out for **6a** and **6b**, that is for the equatorial position of the heteroligand (Figure 1). From previous CCSD(T)/B3LYP studies it is also known that these structures are preferred over the axial ones.^{29a} The optimized parameters of **6a** and **6b** are in good agreement with the experimental data (Table 4). Geometry optimizations for **5a** and **5b** were carried out within the *C*_s-symmetry constraint. In the case of **5a** the structure converges to the *C*_{3v}-symmetric one. Due to a small rotation of the methyl substituents, the *C*_s symmetry of **5b** was retained. Since early X-ray studies showed equal C–C bond lengths in arene rings π-bonded to transition metals,^{43c,e} there was some controversy concerning the symmetry of complexed arenes. For both, **5a** and **5b** we observe the lowering of the 6-fold symmetry of the C₆H₆ and C₆(CH₃)₆ ligands and con-

(38) (a) Michels, G. D.; Fleisch, G. D.; Svec, H. *J. Inorg. Chem.* **1980**, *19*, 479. (b) Wells, J. R.; Weitz, E. *J. Am. Chem. Soc.* **1992**, *114*, 2783. (c) Wells, J. R.; House, P. G.; Weitz, E. *J. Phys. Chem.* **1994**, *98*, 8343. (d) McNamara, B.; Becher, D. M.; Towns, M. H.; Grant, E. R. *J. Phys. Chem.* **1994**, *98*, 4622.

(39) Boned, M. L.; Colomina, M.; Perez-Ossorio, R.; Turrion, C. *Anal. Fisc. Quim. B* **1964**, *60*, 459.

(40) (a) Brown, D. L. S.; Conner, J. A.; Leung, M. L.; Paz-Andrade, M. I.; Skinner, H. A. *J. Organomet. Chem.* **1976**, *110*, 79. (b) House, P. G.; Weitz, E. *J. Phys. Chem. A* **1997**, *101*, 2988.

(41) (a) Ehlers, A. W.; Dapprich, S.; Vydrovichikov, S. F.; Frenking, G. *Organometallics* **1996**, *15*, 105. (b) Dapprich, S.; Frenking, G. *Angew. Chem.* **1995**, *107*, 383.

(42) (a) English, A. M.; Plowman, K. R.; Butler, I. S. *Inorg. Chem.* **1981**, *20*, 2553. (b) Drouin, B. J.; Kukolich, S. G. *J. Am. Chem. Soc.* **1998**, *120*, 6774. (c) McNeill, E. A.; Scholer, F. R. *J. Am. Chem. Soc.* **1977**, *99*, 6243. (d) Drouin, B. J.; Kukolich, S. G. *J. Am. Chem. Soc.* **1999**, *121*, 4023. (e) Davis, M. I.; Speed, S. *J. Organomet. Chem.* **1970**, *21*, 401.

(43) (a) Kukolich, S. G. *J. Am. Chem. Soc.* **1995**, *117*, 5512. (b) Rees, B.; Coppens, P. *Acta Crystallogr. B* **1973**, *29*, 2515. (c) Bailey, M. F.; Dahl, L. F. *Inorg. Chem.* **1965**, *4*, 1314. (d) Byers, B. P.; Hall, M. B. *Inorg. Chem.* **1987**, *26*, 2186. (e) Bailey, M. F.; Dahl, L. F. *Inorg. Chem.* **1965**, *4*, 1298.

sequently the alternating C–C bond lengths in the arene rings. This is in accord with the more accurate and recent experimental studies.^{43a,b,d} The calculated C–C bond length difference in the arene rings amounts to 0.017 Å (**5a**) and 0.020 Å (**5b**) and reproduces almost exactly the experimental values of 0.016 Å (**5a**)^{43a} and 0.021 Å (**5b**).^{43d}

The calculated SCS-MP3 dissociation enthalpies of the heteroligands in **4a–4e** are in excellent agreement with the experimental values (Table 3). As in the case of homoleptic metal carbonyls the corresponding MP2 values are much too high and the MP3 method underestimates the bond strengths. It should be noticed that in the case of **4a–4e** the SCS-MP3 dissociation enthalpies of the heteroligands concur not only with the BP86 results (Table 3) but also with other reported values. Thus, for example, a CCSD(T)//MP2 study on **4a** overestimates the dissociation enthalpy of the thiocarbonyl ligand by 7.6 kcal/mol.^{41a} We suppose, however, that this rather large deviation is due to the poor MP2 structure used in the CCSD(T) studies.^{41a}

For **4b** the measured Cr–Xe bond energy amounts to 9.0 ± 0.9 kcal/mol.^{38b} Like for other strongly bound ligands, the moderate Cr–Xe bond strength has been also rationalized in the frames of the Dewar–Chatt–Duncanson model,⁴⁴ that is, on the basis of synergistic σ -donation and π -back-donation between the ligand and the metal. Taking into account that the Xe atom is polarizable,⁴⁵ as well as the IR spectroscopic information concerning the shift of the carbonyl stretching vibrations, it has been postulated that Xe should be able to donate electron density to the electrophilic metal center.^{38b} It has also been discussed that due to fully occupied orbitals at Xe, back-bonding seems to be not acting in **4b**.^{38b} It is interesting to note that a small enthalpy of 8 ± 2 kcal/mol has also been estimated experimentally for the interaction of CH₄ with Cr(CO)₅.^{38c} The MP2 and SCS-MP2 methods overestimate the dissociation enthalpy of the Xe ligand in **4b** by 5.4 and 1.9 kcal/mol, respectively (Table 3). The SCS-MP3 dissociation enthalpy (7.4 kcal/mol) is slightly smaller than the experimental value (9.0 ± 0.9 kcal/mol),^{38b} while the BP86 result (4.5 kcal/mol) recovers only half of the experimental enthalpy. Since dispersion interactions are expected to be of some importance for this system, the small DFT value (DFT/BP86 provides no binding at all for van der Waals complexes)⁴⁶ seems to be understandable.

The hydrogen molecule in **4c** and **6a** is η^2 bound to the metal center. The experimental enthalpy for H₂ dissociation in **4c** (15.0 ± 1.3 kcal/mol)^{38c} agrees well with the SCS-MP3 or BP86 values of 17.2 and 15.2 kcal/mol, respectively (Table 3). For **6a** the experimental dissociation enthalpy is not known. The computed ΔH^{298} values with our standard triple- ξ basis [20.1 kcal/mol (SCS-MP3), 19.6 kcal/mol (BP86)] compare well with the CCSD(T) result of 18.5 kcal/mol.^{29q} It should be noticed, however, that the use of the quadruple- ξ basis predicts slightly stronger bonding at the SCS-MP3 level (22.4

kcal/mol), while ΔH^{298} from BP86 remains almost unchanged (19.5 kcal/mol). Thus, for **6a** an enhancement of the SCS-MP3 bond strength is observed with increasing saturation of the one-particle basis sets used for calculations. Note that in the CCSD(T) studies basis sets of only valence double- ξ quality were used.^{29q} The greater bonding energy of H₂, as compared to Xe, may be explained by the presence of back-bonding interaction which leads to electron density transfer from occupied metal d-orbitals to the σ^* MO of H₂. As a result, an elongation of the H–H distance from 0.750 Å in the free H₂ to 0.825 and 0.922 Å is observed in **4c** and **6a**, respectively (Table 4). At the BP86 and SCS-MP3 levels the bonding enthalpy of H₂ in **6a** [19.6 kcal/mol (BP86), 20.1 kcal/mol (SCS-MP3)] is greater than that of **4c** by about 3–5 kcal/mol. This suggests that the Fe(CO)₄ fragment provides stronger back-bonding interactions than the Cr(CO)₅ fragment. If this hypothesis is true, then similar trends should be observed for **4d** and **6b**, where the π^* MO of ethylene is populated due to the back-bonding interaction. Upon going from free ethylene to **4d** and **6b**, we observe an elongation of the C–C double bond from 1.333 Å to 1.384 Å (**4d**) and 1.411 Å (**6b**). The experimental enthalpy for the dissociation of ethylene in **4d** was measured as 24.6 ± 3.4 or 25.1 ± 1.0 kcal/mol.^{38c,d} The SCS-MP3 value (25.9 kcal/mol) again agrees very well with experiment. The value from BP86 is significantly smaller (21.6 kcal/mol) (Table 3).

There are different experimental determinations for the enthalpy of ethylene dissociation from **6b**.^{30b,40a,b} Although our SCS-MP3 value (25.2 kcal/mol) agrees well with that from early thermal decomposition experiments (23.1 kcal/mol),^{40a} it is about 10 kcal/mol lower compared to later reports (37.4 kcal/mol^{30b} or 36.0 ± 2.5 kcal/mol^{40b}). The BP86 enthalpy of C₂H₄ dissociation from **6b** (31.6 kcal/mol) is also smaller than the later experimental values. The use of quadruple- ξ basis sets does not introduce significant changes. The BP86 ΔH^{298} value (31.1 kcal/mol) is 0.5 kcal/mol smaller and that from SCS-MP3 (25.3 kcal/mol) differs by only 0.1 kcal/mol from the data obtained with our standard triple- ξ basis. Before the large discrepancies between the different experimental values are resolved, a final assessment of the performance of the theoretical methods for this system is not possible.

In the case of **5a** and **5b**, direct experimental measurements of the strength for the η^6 -bonding of the arene ligands with the Cr(CO)₃ fragment are not known. The presented experimental values in Table 3 were derived from standard enthalpies of formation of the involved species.^{24,39} It is seen that both experimental reaction enthalpies suffer from large uncertainties, and thus a direct comparison with the computed data is problematic. It seems that the BP86 results [58.7 kcal/mol (**5a**), 61.8 kcal/mol (**5b**)] are closer to the experimentally derived ones [59.6 ± 12.3 kcal/mol (**5a**), 66.2 ± 13.7 or 71.7 ± 14.0 kcal/mol (**5b**)], but the SCS-MP3 enthalpies lie also within the experimental error bars. Note, that the SCS-MP3 enthalpies for the bonding of the arene ligands [71.5 kcal/mol (**5a**), 81 kcal/mol (**5b**)] are considerably improved as compared to those from the MP2, MP3, or SCS-MP2 levels [**5a**: 107.1 kcal/mol (MP2), 31.9 kcal/mol (MP3), 90.3 kcal/mol (SCS-MP2);

(44) (a) Dewar, J. S. *Bull. Soc. Chim. Fr.* **1951**, 18, C79. (b) Chatt, J.; Duncanson, L. A. *J. Chem. Soc.* **1953**, 2939.

(45) Hyman, H. H., Ed. *Noble Gas Compounds*; University of Chicago Press: Chicago, 1963.

(46) Grimme, S. *J. Comput. Chem.* **2004**, 25, 1463, and references therein.

Table 5. Theoretically Predicted and Experimentally Derived Enthalpies of the Deprotonation Reactions of Cr(CO)₃C₆H₆ (5a**) and Fe(CO)₃C₄H₆ (**8b**)**

reaction	$\Delta H_R(\text{calc})$ [kcal/mol]					$\Delta H_R(\text{exp})$ [kcal/mol]	ref
	BP86	MP2	MP3	SCS-MP2	SCS-MP3		
5a : Cr(CO) ₃ C ₆ H ₆ → 7 : Cr(CO) ₃ C ₆ H ₅ ⁻ + H ⁺	370.9	366.7	388.8	370.6	376.1	371.8 ± 5.0	47
8b : Fe(CO) ₃ C ₄ H ₆ → 9b : Fe(CO) ₃ C ₄ H ₅ ⁻ + H ⁺	354.5	326.1	435.0	340.2	367.4	340.4 ± 5; <350.0	24, 49
8b : Fe(CO) ₃ C ₄ H ₆ → 9a : Fe(CO) ₃ C ₄ H ₅ ⁻ + H ⁺	373.8	359.1	419.9	368.6	383.8		
8b : Fe(CO) ₃ C ₄ H ₆ → 9c : Fe(CO) ₃ C ₄ H ₅ ⁻ + H ⁺	381.1	345.4	442.1	357.5	381.7		

5b: 122.4 kcal/mol (MP2), 34.4 kcal/mol (MP3), 103.1 kcal/mol (SCS-MP2)] (Table 3).

C. Deprotonation Reactions of Cr(CO)₃C₆H₆ (5a**) and Fe(CO)₃C₄H₆ (**8**).** In this section we present the calculated data on the deprotonation reactions from eqs 8 and 9.



The geometry optimization for the deprotonated complex Cr(CO)₃C₆H₅⁻ (**7**) was carried out without symmetry constraints, but the optimized structure **7** deviates only slightly from C_s symmetry. The optimized bond lengths of **7** are shown in Figure 2.

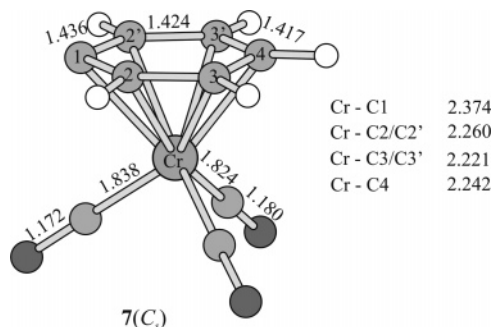


Figure 2. Optimized bond lengths [Å] of Cr(CO)₃C₆H₅⁻ (**7**).

From Figure 2 and Table 4 it is evident that the deprotonation of **5a** affects not only the bond lengths of the benzene ligand but also those of the Cr(CO)₃ group. The acidity of the benzene molecule increases substantially due to the complexation with the Cr(CO)₃ group. This is evident from the experimentally determined gas-phase deprotonation enthalpies for benzene (401.7 kcal/mol) and **5a** (371.5 ± 5.0 kcal/mol).⁴⁷

With the exception of the MP3 result, the BP86, MP2, SCS-MP2, and SCS-MP3 deprotonation enthalpies of **5a** agree well with the experimentally estimated value (Table 5). It should be noticed, however, that in this case the MP2 value (366.7 kcal/mol) is only slightly smaller than the SCS-MP2 result (370.6 kcal/mol), which is closer to experiment (371.5 ± 5 kcal/mol)⁴⁷ than the SCS-MP3 value (376.1 kcal/mol). The geometry optimization for **8** was carried out under the C_s-symmetry constraint. We have considered the two possible rotamers, **8a** and **8b**, shown at the top of Figure 3. According to the vibrational analysis, **8a** has one imaginary frequency and represents the transition state for the rotation of the Fe(CO)₃ group. At the BP86 and SCS-MP3 levels the activation enthalpy for rotation ($\Delta\Delta H^\ddagger$)

of 9.0 and 11.0 kcal/mol, respectively, agrees well with the experimental estimate of 9.1 ± 0.5 kcal/mol^{48a} and with the previous BP86 value of 9.4 kcal/mol.^{48b} Once again the SCS-MP3 result is considerably improved as compared to those from MP2, MP3, and SCS-MP2, which yield $\Delta\Delta H^\ddagger$ values of -0.64, 29.8, and 3.3 kcal/mol, respectively.

To investigate the deprotonation reaction of **8b**, we have considered three deprotonation products, **9a**, **9b**, and **9c**, shown at the bottom of Figure 3. The structures **9a** and **9c** result by removal of the H2 and H1a protons attached to the C2 and C1 butadiene atoms in **8b**, respectively.

It is seen that the optimized structures of **9a** and **9c**, although slightly distorted, show bonding patterns similar to those of **8b**. Removing the H1b proton leads to the rearranged structure **9b**, in which one CO group migrates to the deprotonation side on the C1 butadiene atom. Selected optimized parameters of **8a**, **8b**, and **9a**–**9c** are summarized in Table 6. According to vibrational analyses, **9a**, **9b**, and **9c** represent minima on their potential energy surfaces.

Proton abstraction from **8b** was observed experimentally with several anionic bases with proton affinities (PA) in the range 349.8–372.1 kcal/mol.⁴⁹ On the basis of these experiments the authors were only able to estimate the deprotonation enthalpy of **8b** as being lower than 350 kcal/mol.

Subsequent protonation studies with reference acids suggested that rearrangement of the negative ion Fe(CO)₃C₄H₅⁻ may occur leading to a weaker base than the initially formed conjugate anion.⁴⁹ With the exception of the MP3 method, all other theoretical approaches predict the rearranged ion **9b** as a deprotonation product of **8a** (Table 5, Figure 3). Due to uncertain experimental information, the discussion of the calculated deprotonation enthalpies is rather speculative. However, if we take the deprotonation enthalpy of **8b** from ref 24 (340.4 ± 5 kcal/mol), then the SCS-MP2 result (340.2 kcal/mol) is closest, and the BP86 and SCS-MP3 values are overestimated by 14.1 and 27.0 kcal/mol, respectively (Table 5). The MP2 method underestimates the deprotonation enthalpy of **8b** by 14.3 kcal/mol. As in the case of **5a**, the SCS-MP2 deprotonation enthalpy of **8b** is closer to experiment than the SCS-MP3 value.

D. Protonation Reaction of Ferrocene (10). Although the experimental proton affinity of ferrocene is well known,⁵¹ no structural information is available for the corresponding cation. Depending on the experimental conditions, e.g., solution versus gas-phase and the presence of strong acids versus less protic media, three protonation sites have been suggested, i.e., on the

(47) Lane, K. R.; Squires, R. R. *J. Am. Chem. Soc.* **1985**, *107*, 6403, and references therein.

(48) (a) Kruczynski, L.; Takats, J. *Inorg. Chem.* **1976**, *15*, 3140. (b) Bühl, M.; Thiel, W. *Inorg. Chem.* **1997**, *36*, 2922.

(49) Wang, D.; Squires, R. R. *Organometallics* **1987**, *6*, 905.

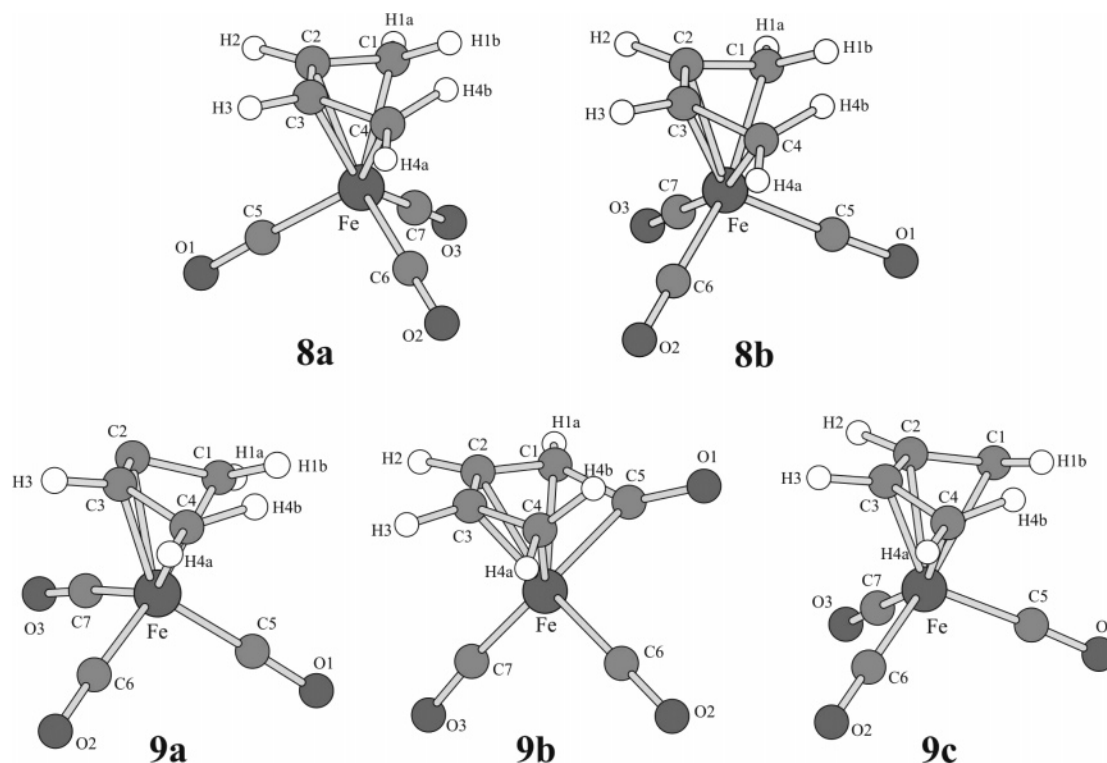


Figure 3. Optimized structures of $\text{Fe}(\text{CO})_3\text{C}_4\text{H}_6$ (**8a**, **8b**) and of the deprotonation products $\text{Fe}(\text{CO})_3\text{C}_4\text{H}_5^-$ (**9a**, **9b**, and **9c**).

Table 6. Optimized Bond Distances [Å] of **8a** and **8b** in Comparison with Available Experimental Data as Well as of **9a**, **9b**, and **9c** and Number of Imaginary Frequencies (NIMAG)

	8a (C_s)		8b (C_s)			9a (C_1)	9b (C_1)	9c (C_1)
	BP86	BP86	X-ray ^a	ED ^b	MW ^c	BP86	BP86	BP86
Fe–C1/Fe–C4	2.173	2.130	2.14	2.084	2.224	2.178/2.121	2.143/2.112	2.367/2.119
Fe–C2/Fe–C3	2.083	2.077	2.06	2.084	2.032	2.150/2.057	2.131/2.088	2.111/2.050
C1–C2/C3–C4	1.418	1.427	1.46	1.409	1.424	1.427/1.435	1.418/1.422	1.429/1.428
C2–C3	1.432	1.420	1.45	1.409	1.406	1.445	1.433	1.442
Fe–C5	1.791	1.786	1.74	1.801	1.776	1.771	1.914	1.783
Fe–C6/Fe–C7	1.766	1.786	1.77	1.801	1.776	1.759/1.793	1.738/1.795	1.760/1.777
C5–O1	1.159	1.157	1.18	1.134	1.149	1.174	1.224	1.168
C6–O2/C7–O3	1.161	1.158	1.13	1.134	1.149	1.174/1.170	1.177/1.179	1.174/1.168
C5–C1		2.840				2.752	1.450	2.698
NIMAG	1 (85i cm^{-1})	0				0	0	0

^a Reference 50a. ^b Gas-phase electron diffraction, ref 50b. ^c Microwave measurements, ref 50c.

metal,^{51,52} on the cyclopentadienyl (Cp),⁵³ or in an agostic position bridging the metal and the protonated carbon of the Cp ring.^{51c} In a deuterium labeling experiment it has been estimated that the protonation at the metal should be at least 5 kcal/mol preferred over the ring protonation.^{51c} A value of about 10 kcal/mol has also been proposed in favor of metal protonation.^{51b} However, other experiments in deuterated media pointed out to a rapid equilibrium between metal- and ring-protonated ferrocene.⁵⁴ It is thus evident that it is

problematic to establish experimentally the preferred protonation side of ferrocene.

Unfortunately, theoretical calculations performed up to now also give contradictory answers on the position of ferrocene protonation.⁵⁵ Thus, for example, at the DFT/BPW91 level the metal-protonated and agostic forms have almost the same energy, and at the DFT/B3LYP level it is the agostic form that is 3.8 kcal/mol more stable.^{55d,e} On the other hand MP2 calculations predict large stabilization of the metal-protonated form (37–42 kcal/mol) over the ring-protonated one.^{55c,e} Like DFT/B3LYP, single-point CCSD(T) studies on BPW91 optimized geometries suggest once again that both forms are close in energy, with the agostic structure being 2.1 kcal/mol more stable.^{55e}

(50) (a) Mills, O. S.; Robinson, G. *Acta Crystallogr.* **1963**, *16*, 758. (b) Davis, M. I.; Speed, S. *J. Organomet. Chem.* **1970**, *21*, 401. (c) Kukulich, S. G.; Roehrig, M. A.; Henderson, G. L.; Wallace, D. W.; Chen, Q.-Q. *J. Phys. Chem.* **1992**, *97*, 829.

(51) (a) Foster, M. S.; Beauchamp, J. L. *J. Am. Chem. Soc.* **1975**, *97*, 4814. (b) Ikonomu, M. G.; Sunner, J.; Kebarle, P. *J. Phys. Chem.* **1988**, *92*, 6308. (c) Meot-Ner, M. *J. Am. Chem. Soc.* **1989**, *111*, 2830.

(52) (a) Curphey, T. J.; Santer, J. O.; Rosenblum, M.; Richards, J. H. *J. Am. Chem. Soc.* **1960**, *82*, 5249. (b) Pavlik, I. J. *Collect. Czech. Chem. Commun.* **1967**, *32*, 76.

(53) (a) Cunningham, A. F., Jr. *J. Am. Chem. Soc.* **1991**, *113*, 4864.

(b) *Organometallics* **1994**, *13*, 2480. (c) *Organometallics* **1997**, *16*, 1114.

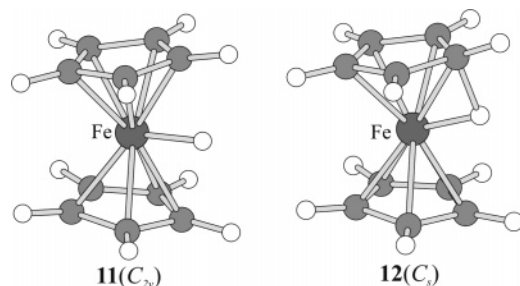
(54) Müller-Westerhoff, U. T.; Haas, T. J.; Swiegers, G. F.; Leipert, T. K. *J. Organomet. Chem.* **1994**, *472*, 229.

(55) (a) Weber, J.; Fluekiger, P.; Stussi, D.; Morgantini, P. Y. *THEOCHEM* **1991**, *227*, 175. (b) Jungwirth, P.; Stussi, D.; Weber, J. *Chem. Phys. Lett.* **1992**, *190*, 29. (c) McKee, M. L. *J. Am. Chem. Soc.* **1993**, *115*, 2818. (d) Mayor-López, M. J.; Weber, J.; Mannfors, B.; Cunningham, A. F., Jr. *Organometallics* **1998**, *17*, 4983. (e) Mayor-López, M. J.; Lüthi, H. P.; Koch, H.; Morgantini, P. Y. Weber, J. *J. Chem. Phys.* **2000**, *113*, 8009.

Table 7. Optimized Bond Distances [Å] of $11(C_{2v})$ and $12(C_s)$ in Comparison with Previous Studies

	method	Fe–H ⁺	Fe–C	C–C	C–H	C–H ⁺	ref
$11(C_{2v})$	HF	1.618	2.079–2.194	1.381–1.452			55c
	MP2	1.586	2.005–2.162	1.439–1.490			55c
	LDA	1.488	2.032–2.041	1.414–1.431	1.090–1.093	1.822	55d
	BPW91	1.495	2.080–2.093	1.424–1.442	1.085–1.087	1.879	55d
	BP86	1.495	2.074–2.083	1.423–1.442	1.085–1.087	1.868	this work
$12(C_s)$	BPW91	1.561	2.032–2.102	1.416–1.468	1.086–1.091	1.422	55d
	BP86	1.585	2.035–2.100	1.414–1.471	1.085–1.093	1.361	this work

In our investigations we have considered the C_{2v} -symmetric isomer (**11**) for metal-protonated ferrocene and a C_s -symmetric structure for the ring-protonated form. During the geometry optimizations the ring-protonated ferrocene converged to the agostic structure (**12**) (Figure 4).

**Figure 4.** Optimized structures of metal- (**11**) and ring- (agostic) protonated ferrocene (**12**).

From previous DFT calculations it is known that among the possible isomers for metal- and ring-protonated ferrocene, **11**(C_{2v}) and **12**(C_s) represent the most stable ones.⁵⁵ Since in **11**(C_{2v}) and **12**(C_s) the Cp ligands adopt eclipsed conformations, proton affinities were calculated with respect to the D_{5h} structure of ferrocene (**10**). The optimized Fe–C, C–C, and C–H bond lengths of **10**(D_{5h}) are 2.056, 1.434, and 1.085 Å, respectively, and agree well with the corresponding experimental gas-phase distances of 2.064, 1.440, and 1.104 Å.⁵⁶ Selected optimized parameters of **11**(C_{2v}) and **12**(C_s) are compared with previous theoretical data in Table 7. From Table 7 it is seen that our BP86 optimized parameters of **11**(C_{2v}) and **12**(C_s) are almost the same as those derived in previous BPW91 studies.^{55d} The C–H⁺ distance of the agostic structure **12**(C_s) (1.361 Å) is largely stretched as compared with the other C–H bonds (1.085–1.093 Å), and the Fe–H⁺ distance is 0.090 Å longer than in metal-protonated ferrocene, **11**(C_{2v}).

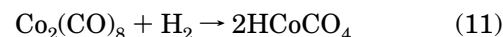
It is interesting to note that, on the basis of experimental and theoretical studies, agostic interactions were also postulated to stabilize the ground state structure of isoelectronic neutral (borole)(cyclopentadienyl)hydridoiron derivatives as well as of the closely related protonated half-open ruthenocenes.⁵⁷ Furthermore, for both types of complexes an intramolecular proton transfer was monitored by temperature-dependent NMR spectra.⁵⁷

According to the definition, the gas-phase proton affinity (PA) of molecules is equal to the negative value of the enthalpy for the protonation reaction at room

temperature (PA = $-\Delta H^{298}$). The calculated PAs for the metal, **11**(C_{2v}), and the agostic structure, **12**(C_s), of protonated ferrocene are collected in Table 8. As in the BPW91 studies,^{55d} the calculated PAs at the BP86 level of **11**(C_{2v}) and **12**(C_s) are very close in energy, although we obtain here a slight preference (0.3 kcal/mol) for metal protonation. As mentioned previously, MP2 prefers metal protonation, but the calculated PAs of **11**(C_{2v}) range from 246 to 251 kcal/mol and are largely overestimated as compared to the experimental values (206–213 kcal/mol) (Table 8). Furthermore, the high preference for metal over ring protonation of 37–42 kcal/mol seems to contradict the experimentally observed equilibrium between metal- and ring-protonated ferrocene.

Upon going from MP2 to SCS-MP2, and further to SCS-MP3, the preference for metal protonation diminishes from 37.5 kcal/mol (MP2) to 28.0 kcal/mol (SCS-MP2), and 10.9 kcal/mol (SCS-MP3). At the SCS-MP3 level the calculated PAs for **11**(C_{2v}) of 214.8 kcal/mol and for **12**(C_s) of 203.9 kcal/mol agree well with the experimental values⁵¹ and do not exclude the dynamic behavior of protonated ferrocene.

E. Hydrogenation Reaction of $Mn_2(CO)_{10}$ (13**) and $Co_2(CO)_8$ (**15**).** $Mn_2(CO)_{10}$ (**13**) is the only isolable homoleptic manganese carbonyl, while $Co_2(CO)_8$ is the simplest closed-shell cobalt carbonyl. Both complexes undergo hydrogenation reaction (eqs 10 and 11), and the corresponding reaction enthalpies were measured in solution.⁵⁸



The geometry optimizations for **13** were carried out within the C_s -symmetry constraint. During the geometry optimization **13**(C_s) converged to the staggered structure of D_{4d} symmetry. This is in accord with X-ray diffraction data⁵⁹ as well as with previous theoretical studies, which showed that the staggered **13**(D_{4d}) structure is lower in energy than the eclipsed **13**(D_{4h}) one.⁶⁰ According to the 18 valence electron rule,⁶¹ both **13**(D_{4d}) and **13**(D_{4h}) are characterized by a single Mn–Mn bond.

(58) (a) Klingler, R. J.; Rathke, J. W. *Inorg. Chem.* **1992**, *31*, 804. (b) Bor, G. *Pure Appl. Chem.* **1986**, *58*, 543. (c) Rathke, J. W.; Klingler, R. J.; Krause, T. R. *Organometallics* **1992**, *11*, 585. (d) Ungwary, F. J. *Organomet. Chem.* **1972**, *36*, 363.

(59) (a) Almenninger, A.; Jacobsen, G. G.; Seip, H. M. *Acta Chem. Scand.* **1969**, *23*, 685. (b) Dahl, L. F.; Rundle, R. E. *Acta Crystallogr.* **1963**, *16*, 419. (c) Martin, M.; Rees, B.; Mitschler, A. *Acta Crystallogr.* **1981**, *338*, 6.

(60) (a) Folga, E.; Ziegler, T. *J. Am. Chem. Soc.* **1993**, *115*, 5169. (b) Xie, Y.; Jang, J. H.; King, R. B.; Schaefer, H. F., III. *Inorg. Chem.* **2003**, *42*, 5219. (c) Kenny, J. P.; King, R. B.; Schaefer, H. F., III. *Inorg. Chem.* **2002**, *40*, 900.

(61) Albright, T. A.; Burdett, J. K.; Whangbo, M.-H. *Orbital Interactions in Chemistry*; Wiley: New York, 1985; pp 298–304.

(56) Haaland, A. *Acc. Chem. Res.* **1979**, *12*, 415.

(57) (a) Herberich, G. E.; Carstensen, T.; Köffer, D. P. J.; Klaff, N.; Boese, R.; Hyla-Kryspin, I.; Gleiter, R.; Stephan, M.; Meth, H.; Zenneck, U. *Organometallics* **1994**, *13*, 619. (b) Trakarnpruk, W.; Hyla-Kryspin, I.; Arif, A. M.; Gleiter, R.; Ernst, R. D. *Inorg. Chim. Acta* **1997**, *259*, 197.

Table 8. Comparison of Calculated Proton Affinities (PA) for Metal-Protonated, 11(C_{2v}), and Agostic, Ring-Protonated, 12(C_s), Structures of Ferrocene with Previous Theoretical and Experimental Data as Well as Relative Enthalpies ($\Delta\Delta H^{298}$) of the Protonation Reactions

method	PA [kcal/mol]		$\Delta\Delta H^{298}$ [kcal/mol] ^a	ref
	11(C_{2v})	12(C_s)		
HF	172.9	197.3	-24.4	55e
	173.9	193.3	-19.4	this work
	165.9	178.2	-12.3	55c
MP2	167.6	220.0 ^b	-52.4	55c
	250.9	208.9	+42.0	55c
	246.5	209.3	+37.2	55e
MP3	246.3	208.8	+37.5	this work
	158.0	189.7	-31.7	this work
SCS-MP2	236.7	208.7	+28.0	this work
SCS-MP3	214.8	203.9	+10.9	this work
CCSD	208.9	213.8	-4.9	55e
CCSD(T)	215.6	217.7	-2.1	55e
BPW91	211.0	212.0	-1.0	55d
BP86	211.9	211.6	+0.3	this work
expt	213.0 ± 4.5;			51a,b,c
	205.9 ± 1.5; 207.0 ± 1.0			

^a $\Delta\Delta H^{298} = \Delta H^{298}[12(C_s)] - \Delta H^{298}[11(C_{2v})]$. ^b For purely ring-protonated ferrocene, without agostic interaction.

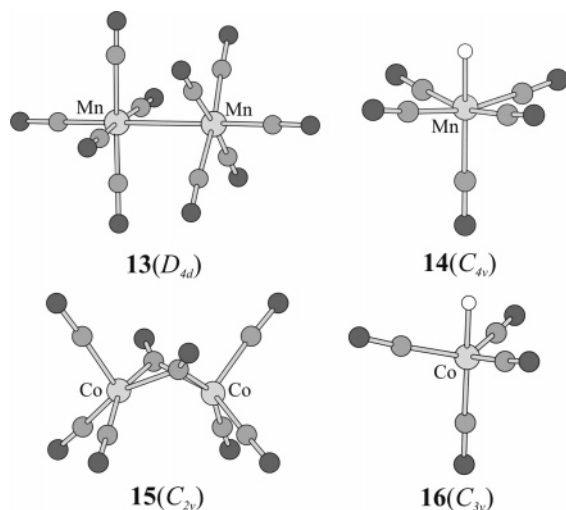


Figure 5. Optimized structures of $Mn_2(CO)_{10}$ (**13**) and $Co_2(CO)_8$ (**15**) and their hydrogenation reaction products $HMn(CO)_5$ (**14**) and $HCo(CO)_4$ (**16**).

From X-ray diffraction⁶² and IR spectroscopic studies⁶³ it is known that **15** can adopt different geometric structures. Our calculations were carried out for the dibridged C_{2v} -symmetric isomer without Co–Co bonding, which according to previous calculations represents the most stable structure.^{60a,c} The optimized structures of **13**(D_{4d}) and **15**(C_{2v}) together with their hydrogenation reaction products, $HMn(CO)_5$ (**14**) and $HCo(CO)_4$ (**16**), are shown in Figure 5.

14 adopts a distorted square-bipyramidal structure with C_{4v} symmetry, and **16** converges to a pseudo-

Table 9. Optimized Bond Distances [Å] of 13–16 in Comparison with Experimental and Previous Theoretical Data

	method	Mn–Mn	Mn–C _{ax}	Mn–C _{eq}	ref
$Mn_2(CO)_{10}$ 13 (D_{4d})	LDA/NL	2.902	1.813	1.859	60a
	B3LYP	3.007	1.814	1.864	60b
	BP86	2.954	1.803	1.851	60b
		2.979	1.807	1.855	this work
	expt	2.977	1.803	1.873	59a
		2.923	1.792	1.830	59b
		2.895	1.820	1.859	59c
	method	Co–Co	Co–C _t	Co–C _b	ref
$Co_2(CO)_8$ 15 (C_{2v})	LDA/NL	2.592	1.825	1.974	60a
	B3LYP	2.557	1.827/1.820	1.955	60c
	BP86	2.550	1.813/1.805	1.957	60c
		2.551	1.818/1.809	1.961	this work
expt	2.528	1.827	1.939	62a	
				62b	
				62c	
	method	M–H	M–C _{ax}	M–C _{eq}	ref
$HMn(CO)_5$ 14 (C_{4v})	LDA/NL	1.589	1.854	1.855	60a
	BP86	1.574	1.848	1.846	this work
	expt	1.576	1.854	1.856	64
$HCo(CO)_4$ 16 (C_{3v})	LDA/NL	1.499	1.803	1.801	60a
	BP86	1.487	1.803	1.794	this work
	expt	1.556	1.764	1.818	64

trigonal-bipyramidal structure with C_{3v} symmetry. In both, **14** and **16**, the equatorial CO groups are slightly bent toward the axial hydrogen. The optimized parameters of **13**–**16** are compared with available experimental and previous theoretical data in Table 9.

The BP86 optimized structure of **13**(D_{4d}) agree well with the experimental data (Table 9). It should be noticed that in the case of $Co_2(CO)_8$ the reported crystal structures⁶² do not distinguish between the two different types of terminal carbonyls. Thus, a precise comparison between theory and experiment is not possible. According to B3LYP or BP86 calculations, the differences in terminal Co–C distances are in the range 0.007–0.009 Å (Table 9). The BP86 Mn–H distance of **14**(C_{4v}) (1.574 Å) agrees well with the experimental value (1.576 Å), but the Co–H distance of **16**(C_{3v}) is found to be 0.069 Å shorter than in the experiment.

Similar features were also obtained in other DFT studies, where the optimized Co–H distance was found to be 0.057 Å shorter than the experimental values.^{60a} We agree with the opinion of these authors, that most of the deviation in the Co–H distance may be due to experimental uncertainties, since it is in general difficult to locate hydrogen next to the metal in electron diffraction studies.^{60a}

The computed enthalpies of hydrogenation reaction of **13**(D_{4d}) and **15**(C_{2v}), together with experimental values, are collected in Table 10.

To our best knowledge, only one theoretical study has been undertaken on these reactions.^{60a} In the case of the cobalt carbonyl (**15**) our BP86 result (4.0 kcal/mol) is closer to experiment (3–4 kcal/mol)⁵⁸ than that from LDA (6.6 kcal/mol).^{60a} For the manganese complex **13**, the BP86 result (1.7 kcal/mol) is much smaller than the LDA value (9.7 kcal/mol)^{60a} and is in error by about 7 kcal/mol compared with the experimental enthalpy of 8.7 ± 0.3 kcal/mol^{58a} (Table 10). This finding and the strong functional dependence of the results underline the complexity of this reaction. From Table 10 it is

(62) (a) Leung, P. C.; Coppens, P. *Acta Crystallogr.* **1983**, *B39*, 535. (b) Sunner, G. G.; Klug, H. P.; Alexander, L. E. *Acta Crystallogr.* **1964**, *17*, 732. (c) Braga, D.; Grepioni, F.; Sabatino, P.; Gavezotti, A. *J. Chem. Soc., Dalton. Trans.* **1992**, 1185.

(63) (a) Noack, K. *Spectrochim. Acta* **1963**, *19*, 1925. (b) Koelle, U. In *Encyclopedia of Inorganic Chemistry*; King, R. D., Ed.; Wiley: Chichester, England, 1994; pp 733–747. (c) Brienne, S. H. R.; Markwell, R. D.; Barnett, S. M.; Butler, I. S.; Finch, J. A. *Appl. Spectrosc.* **1993**, *47*, 1131.

(64) McNeill, E. A.; Scholer, F. R. *J. Am. Chem. Soc.* **1977**, *99*, 6243.

Table 10. Calculated and Experimental Enthalpies [kcal/mol] for the Hydrogenation Reaction of **13(D_{4d}) and **15**(C_{2v}) According to Eqs 10 and 11, Respectively**

method	$Mn_2(CO)_{10} - \mathbf{13}(D_{4d})$	$Co_2(CO)_8 - \mathbf{15}(C_{2v})$
LDA	9.7 ^a	6.6 ^a
BP86	1.7	4.0
MP2	21.8	40.6
MP3	-13.8	-56.4
SCS-MP2	14.7	27.3
SCS-MP3	5.8	3.0
expt	8.7 ± 0.3^b	$3.1 \pm 0.2^c; 4.0 \pm 0.2^d; 3.2^e$

^a Reference 60a. ^b Reference 58a. ^c Reference 58b. ^d Reference 58c. ^e Reference 58d.

evident that MP2, MP3, and SCS-MP2 predict unreliable values for both reactions, although it should be mentioned that SCS-MP2 represents also in these cases an improvement compared to standard MP2. The SCS-MP3 hydrogenation enthalpies of 5.8 kcal/mol (**13**) and 3.0 kcal/mol (**15**) agree well with experiment and furthermore predict the right qualitative picture; that is, hydrogenation of **13** is more endothermic than of **15**. This once again confirms the capability of this method to provide reliable and accurate values for the thermochemistry of organometallic compounds.

Conclusions

The present studies indicate that the erratic behavior of the MP n methods concerning thermochemical data of the first-row transition metal compounds can be corrected by improved calculation of the electron correlation effects within the spin component scaled perturbation theory SCS-MP2 and SCS-MP3. The set of systems studied covers different types of chemical bonding and a broad range of reaction enthalpies (from a few kcal/mol to a few hundred kcal/mol), and thus, it may be regarded as a good benchmark for quantum chemical calculations. It has previously been shown that SCS-MP2 significantly improves results for molecules composed from light elements and especially for cases with complicated electronic structures. This holds also for the present studies; that is, SCS-MP2 is superior over MP2 for every reaction, but satisfactory accuracy was achieved only in cases where metal electrons are not directly disturbed by the reaction. The SCS-MP2 enthalpies of the deprotonation reactions of **5a** and **8b**

differ by no more than 1.2 kcal/mol from the experimental values. For all other investigated reactions remarkably good agreement with experimental data was obtained with SCS-MP3, that is, after accounting for spin-independent damping of the third-order correlation energy term. Physically, the importance of some third-order terms for TM compounds is understandable. They introduce couplings between the electron pair excitations that are necessary when many electrons are close together as, for example, in TM atoms and their compounds. The average deviations from experimental dissociation enthalpies of the carbonyl ligands in complexes **1–3** are found to be 19.3 kcal/mol (MP2), 29.8 kcal/mol (MP3), 9.6 kcal/mol (SCS-MP2), 3.7 kcal/mol (SCS-MP3), and 4.5 kcal/mol (DFT/BP86). Similar improvements by SCS-MP3 (as compared to standard MP n treatments) were also obtained for the dissociation processes of the heteroligands from **4–6**, for which the average deviation are 21.6 kcal/mol (MP2), 16.4 kcal/mol (MP3), 13.2 kcal/mol (SCS-MP2), 4.5 kcal/mol (SCS-MP3), and 2.4 kcal/mol (DFT/BP86). The SCS-MP3 proton affinities for metal-protonated ferrocene (214 kcal/mol) and the agostic ring-protonated form (203.9 kcal/mol) agree well with the experimental values (206–213 kcal/mol) and, opposite of MP2, do not exclude dynamic behavior of protonated ferrocene. For **15**, both SCS-MP3 and DFT/BP86 calculate the enthalpy of the hydrogenation reaction with high accuracy, but in the case of **13** the SCS-MP3 enthalpy (5.8 kcal/mol) agrees better with experiment (8.7 ± 0.3 kcal/mol) than the DFT/BP86 value (1.7 kcal/mol). Our standard basis set of triple- ξ quality is saturated enough for DFT/BP86; that is, use of extended basis sets of quadruple- ξ quality does not change significantly the accuracy of the calculated data. However, as desirable for a good quantum chemical method, for SCS-MP3 an increase of the accuracy with better basis sets can be obtained. The SCS-MP3 dissociation reaction enthalpies of **1c** and **3a** were corrected in the right direction, that is, the deviation from experiment diminished from 3.1 kcal/mol to 0.6 kcal/mol for **1c** and from 7.4 kcal/mol to 4.3 kcal/mol for **3a**. For complex chemical systems including transition metals, simultaneous application of DFT and SCS-MP3 methods may be helpful to increase the reliability of the predictions.

OM049521B